Experimental Evidence of Reduced Plasma Flow Damping with Quasisymmetry

S. P. Gerhardt,* J. N. Talmadge, J. M. Canik, and D. T. Anderson

Department of Electrical and Computer Engineering, University of Wisconsin–Madison, Madison, Wisconsin, USA
(Received 11 May 2004; published 7 January 2005)

Measurements of plasma flow damping have been made in the helically symmetric experiment using a biased electrode to impulsively spin the plasma. There are two time scales in the evolution of the plasma flow, for both the spin-up and relaxation. Compared to a configuration with the quasisymmetry broken, the flow in the quasisymmetric configuration rises more slowly and to a higher value at bias turn-on, and decays more slowly at bias turn-off. The decays of the flows are significantly faster than the neoclassical prediction.

A new generation of stellarators has been developed that exploit the concept of quasisymmetric magnetic fields [1]. These configurations are predicted to have reduced viscous damping of plasma flows in the direction of symmetry, in a fashion similar to the small neoclassical damping of toroidal flows in a tokamak. This is in contrast to conventional stellarators, where the complicated structure of $|B|$ on a magnetic surface leads to large viscous damping of flows in all directions on the surface. It has been argued that lower viscosity in future quasisymmetric stellarators [2] may lead to larger flow shear that can help suppress anomalous transport and lead to enhanced confinement regimes, similar to the way toroidal flows and flow shear are known to improve confinement in axisymmetric devices [3]. Hence, it is important to experimentally verify the reduced damping of flows in stellarators with quasisymmetry. In this Letter we present the first results which show that manipulation of the plasma boundary and the resulting magnetic field spectrum in a stellarator to achieve quasisymmetry lead to a reduction in plasma flow damping.

Studies of flow damping in conventional stellarators have demonstrated the importance of both neoclassical and anomalous flow damping. Experiments in CHS showed that, in configurations with significant neoclassical toroidal viscosity, the damping of toroidal flows is approximately neoclassical [4]. In configurations where the toroidal viscosity is reduced, anomalous viscosity is needed to explain the flow damping. Similar results were observed in W7-AS [5]. Measurements in the small stellarator IMS showed good agreement of the measured radial conductivity and flow decay rates [6] with the neoclassical model of Coronado and Talmadge [7].

This Letter presents measurements of the flow evolution in the quasisymmetric stellarator helically symmetric experiment (HSX) [8]. It is shown for the first time that the plasma responds to the bias with a two time-scale flow evolution when a biased electrode is used to impulsively spin the plasma. A neoclassical model for the spin-up is presented based on the observed floating potential, plasma flow, and electrode current evolution. It is shown that the damping is reduced in the quasisymmetric configuration

compared to a configuration with broken symmetry, but that the decay rate of plasma flows is generally larger than the neoclassical prediction.

The main quasihelically symmetric field of HSX is generated with 48 nonplanar coils; a set of 48 planar trim coils can be used to break the quasisymmetry. The magnetic field of the stellarator is described using Hamada coordinates [9], a nonorthogonal coordinate system defined such that the magnetic field and equilibrium current density are both straight lines. The various magnetic configurations of HSX are described by their Fourier decomposition in this coordinate system, given by

$$B = B_0 \sum_{n,m} b_{nm} \cos(m\alpha - n\zeta), \qquad (1)$$

where α is the Hamada poloidal angle and ζ is the Hamada toroidal angle, and m and n are the poloidal and toroidal mode numbers, respectively. The spectrum in the quasihelically symmetric (QHS) configuration is dominated by a single helical component with mode numbers $(n, m) = (4, 1)$. In the mirror configuration, a spectral component with mode numbers $(n, m) = (4, 0)$ and amplitude similar to the helical component breaks the quasisymmetry. This configuration is predicted to have significantly larger viscous damping than the QHS configuration, although the two configurations have similar magnetic surface shape, rotational transform, well depth, and volume.

To generate plasma flow in HSX, we use an electrode inserted inside the last closed magnetic surface to draw a radial current through the plasma. This radial current exerts a $\mathbf{J} \times \mathbf{B}$ torque on the plasma, providing a drive for the plasma rotation. A bias voltage of $\sim$350 V is applied to the electrode in $\sim$1 μs at the initiation of the bias, and an electrode current of typically $\sim$10 A is terminated in $\sim$1 μs when the bias is turned off. To measure the flows induced by the electrode bias, a pair of six-tip Mach probes [10] have been constructed. These probes are capable of simultaneously measuring poloidal and toroidal flows with $\sim$15 μs time resolution. All flow measurements from these probes will be presented in terms of Mach number, defined as $M = V_f / \sqrt{T_e/m_i}$, where V_f is the plasma flow

speed, T_e is the electron temperature, and m_i is the ion mass. The probes have an additional seventh tip used to measure the floating potential.

All discharges discussed in this Letter are produced using 50 kW of 2nd harmonic electron cyclotron heating (ECH) at 28 GHz with a magnetic field $B = 0.5$ T. The line average plasma density was $\sim 1 \times 10^{12}$ cm^{-3}. Doppler spectroscopic measurements of O^{+4} ions indicate an impurity temperature of ~ 20 eV in both the QHS and mirror configurations. This impurity ion temperature should be close to the majority proton temperature due to the tight collisional coupling. Ions at this temperature are in the plateau regime. Arrays of H-alpha detectors [11] are used to estimate the neutral hydrogen density.

The typical evolution of the electrode voltage and current, floating potential, and plasma flow is shown in Fig. 1. The biased electrode was inserted 3 cm inside the last closed magnetic surface to $r/a \sim 0.65$, while the Mach probe was situated at $r/a \sim 0.85$. The electrode voltage and the floating potential at the Mach probe rise at the same fast rate. There is a large spike in the electrode current before it settles to a steady value. The figure also shows the flow (in Mach number) broken into two components: the flow which is approximately parallel to the magnetic field and the flow which is perpendicular to the magnetic field but in the magnetic surface. The perpendicular component of the flow grows at a rate (inverse time constant) of greater than 100 kHz, which is faster than the probes can accurately measure. The parallel flow shows that there is a slower rate for a second component of the flow to grow, corresponding to ~ 2 kHz in this case. Note that both the slow and fast rates contribute to both the parallel and perpendicular flow evolution. The spin-down process is initiated by the open circuiting of the electrode current. The electrode voltage (which is simply a floating potential monitor once the current is broken) and floating potential at
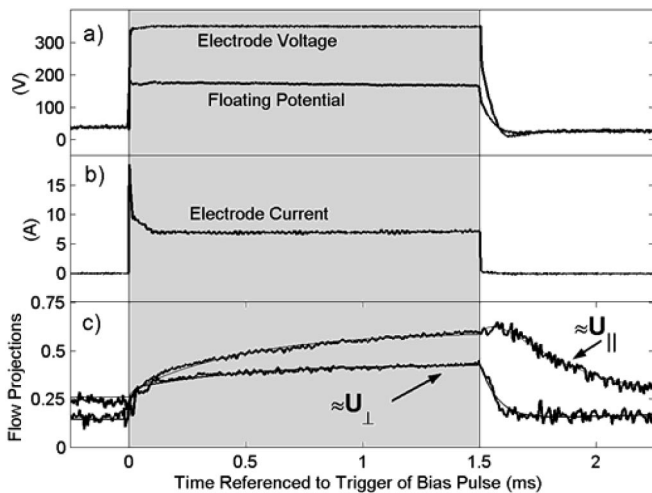
the Mach probe both decay at a rate of ~ 25 kHz. The perpendicular component of the flow decays on a similar time scale, leaving behind only parallel flow. This parallel flow relaxes to the state before the bias pulse at a rate of ~ 5 kHz. Two rates are observed in the flow evolution for both the spin-up and spin-down phases.

A fit technique has been developed to extract the flow evolution rates from these data. It is assumed that the flow rises with a fast rate (r_F) in a direction **f** and a slower rate (r_s) in a direction **s**.

$$\mathbf{U}(t) = C_f[1 - \exp(-r_f t)]\mathbf{f} + C_s[1 - \exp(-r_s t)]\mathbf{s}. \quad (2)$$

The rates (r_F and r_s), directions (**f** and **s**), and flow magnitudes (C_f and C_s) are used as free parameters when fitting (2) to the vector flow measurement. A second step is used to fit the decay with the substitution in (2): $1 - \exp(-rt) \rightarrow \exp(-rt)$.

These studies have been made in otherwise similar QHS and mirror discharges. The total flow speed evolution is shown for representative QHS and mirror discharges in Fig. 2. These two discharges have the same line averaged density and ECH power, the electrode and probes are at similar locations, and the electrode voltage was ~ 340 V in both cases. The two waveforms have a similar initial rise, after which the QHS waveform continues to climb even as the mirror waveform saturates at a lower level. The flow rises at a slower rate in the QHS configuration ($r_s \approx 1.8$ kHz) compared to the mirror case ($r_s \approx 3.5$ kHz) and the maximum flow speed is larger for the QHS configuration. The current drawn by the electrode in steady state was 8 A in the QHS configuration, while the value for the mirror configuration was 10 A. Hence, the QHS configuration has approximately 3 times as much flow for the same $\mathbf{J} \times \mathbf{B}$ torque.

HSX is not perfectly quasisymmetric; there are small symmetry breaking spectral components that lead to neoclassical viscous damping in the quasisymmetric configuration. Furthermore, the low-density plasma is essentially transparent to atomic hydrogen. Quantifying the effects of the neutrals and field ripples on the flow damping is the

FIG. 1. Evolution during and after the electrode pulse of (a) the electrode voltage and floating potential, (b) the electrode current, (c) the Mach number of the approximately parallel and perpendicular plasma flows, for the QHS configuration.
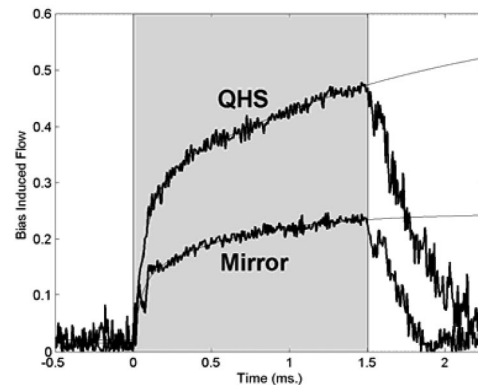
FIG. 2. Comparison of the flow evolution in the QHS and mirror configurations. Flow speeds are in terms of the Mach number.

goal of our neoclassical modeling. In the model used in this research, the poloidal and parallel momentum equations

$$m_i N_i \frac{\partial}{\partial t}\langle \mathbf{B} \cdot \mathbf{U}\rangle = -\langle \mathbf{B} \cdot \nabla \cdot \Pi\rangle - m_i N_i v_{\text{in}}\langle \mathbf{B} \cdot \mathbf{U}\rangle, \quad (3)$$

$$m_i N_i \frac{\partial}{\partial t}\langle \mathbf{B}_P \cdot \mathbf{U}\rangle = -\frac{\sqrt{g}B^\zeta B^\alpha}{c}\langle \mathbf{J}_{\text{plasma}} \cdot \nabla\psi\rangle$$
$$- \langle \mathbf{B}_P \cdot \nabla \cdot \Pi\rangle - m_i N_i v_{\text{in}}\langle \mathbf{B}_P \cdot \mathbf{U}\rangle \quad (4)$$

are solved on each flux surface independently. In these expressions, N_i is the ion density, U is the flow speed, v_{in} is the ion-neutral collision frequency, $\mathbf{B}_P = B^\alpha \mathbf{e}_\alpha$ is the Hamada poloidal field, B^α and B^ζ are the contravariant poloidal and toroidal magnetic fields, $\mathbf{e}_\alpha$ is the covariant poloidal basis vector, ψ is the toroidal flux, $\sqrt{g}$ is the Jacobian, and c is the speed of light. $\mathbf{J}_{\text{plasma}}$ is the current flowing through the plasma across the magnetic surfaces, and is equal to the external (electrode) current in steady state. The ion temperature gradient is neglected in this model. The neoclassical viscosities in (3) and (4) can be written in the plateau regime [12] as $\langle \mathbf{B} \cdot \nabla \cdot \Pi\rangle = \mu_\alpha U^\alpha + \mu_\zeta U^\zeta$ and $\langle \mathbf{B}_P \cdot \nabla \cdot \Pi\rangle = \mu_\alpha^{(P)} U^\alpha + \mu_\zeta^{(P)} U^\zeta$, where $\mu_\alpha = \kappa(B^\alpha \alpha_P + B^\zeta \alpha_\zeta)$, $\mu_\zeta = \kappa(B^\alpha \alpha_C + B^\zeta \alpha_T)$, $\mu_\alpha^{(P)} = \kappa B^\alpha \alpha_P$, and $\mu_\zeta^{(P)} = \kappa B^\alpha \alpha_C$. These expressions in turn use $\kappa = \pi^{1/2}PB_o/v_t B^\zeta$, $\alpha_T = \sum n^2 b_{n,m}^2/|n - m\iota|$, $\alpha_P = \sum m^2 b_{n,m}^2/|n - m\iota|$, and $\alpha_c = -\sum nmb_{n,m}^2/|n - m\iota|$, where P is the pressure and v_t is the thermal velocity and the sums are over all spectral components except the $(n, m) = (0, 0)$ component. Strictly speaking, these expressions for the viscosity are only valid for time scales longer than the ion-ion collision time [13] ($\tau_{ii} \approx 100\ \mu$s in present HSX plasmas).

Based on the experimental observations, we have developed a new model to explain the spin-up process [14]. In keeping with the observations in Fig. 1, the modeled spin-up is driven by a quick rise of the electric field. Radial force balance indicates that $\mathbf{E} \times \mathbf{B}$ flows will grow at the rate that the electric field is applied, and incompressibility of the ion fluid leads to compensating Pfirsch-Schlueter like flows growing at the same rate. The parallel momentum balance shows that a second component of the flow grows in the parallel direction at a "hybrid" rate v_F determined by the damping rates in both the toroidal and poloidal directions: $v_F = \iota v_\alpha + v_\zeta + v_{\text{in}}$, where $v_\alpha = \mu_\alpha B^\zeta/m_i n_i\langle B^2\rangle$ is a poloidal damping frequency and $v_\zeta = \mu_\zeta B^\zeta/m_i n_i\langle B^2\rangle$ is a toroidal damping frequency.

To model the decay of the plasma parameters, we follow the formulation of Coronado and Talmadge [7] in which the external current is turned off extremely quickly to initiate the spin-down. The modeling predicts that there will be two rates for the decay of the flows and electric field, given by

$$\left.\begin{matrix}\gamma_1 \\ \gamma_2\end{matrix}\right\} = -v_{\text{in}} - \frac{v_1 - I_o v_{\text{in}}}{2\Omega} \pm \left[\left(\frac{v_1 - I_o v_{\text{in}}}{2\Omega}\right)^2\right.$$
$$\left. + \frac{v_{\text{in}}I_o(\iota v_\alpha + v_\zeta) + v_\zeta^{(P)} v_\alpha - v_\alpha^{(P)} v_\zeta}{\Omega}\right]^{1/2}, \quad (5)$$

where $I_o = (B^\alpha B^\zeta/2\pi)^2\langle \nabla\rho \cdot \nabla\rho\rangle/(4\pi m_i N_i\langle \mathbf{B}_p \cdot \mathbf{B}_p\rangle)$ and $\Omega = 1 + I_o - \langle \mathbf{B} \cdot \mathbf{B}_p\rangle^2/(\langle \mathbf{B}_p \cdot \mathbf{B}_p\rangle\langle \mathbf{B} \cdot \mathbf{B}\rangle)$. The viscous frequencies are defined as $v_\alpha^{(P)} = \mu_\alpha^{(P)} B^\alpha/m_i N_i\langle \mathbf{B}_p \cdot \mathbf{B}_p\rangle$ and $v_\zeta^{(P)} = \mu_\zeta^{(P)} B^\alpha/m_i N_i\langle \mathbf{B}_p \cdot \mathbf{B}_p\rangle$, and the frequency v_1 is given by

$$v_1 = v_\alpha^{(P)} + (1 + I_o)(\iota v_\alpha + v_\zeta) - \frac{\langle \mathbf{B} \cdot \mathbf{B}_P\rangle}{\langle \mathbf{B} \cdot \mathbf{B}\rangle}(v_\alpha^{(P)}$$
$$+ qv_\zeta^{(P)}) - \frac{\langle \mathbf{B} \cdot \mathbf{B}_P\rangle}{\langle \mathbf{B}_P \cdot \mathbf{B}_P\rangle}\iota v_\alpha. \quad (6)$$

The slower rate corresponds to the damping of plasma flow in the direction of symmetry [14], and goes to zero in the limit of perfect quasisymmetry with no neutrals.

The three rates for the QHS and mirror configurations of HSX are shown in Fig. 3 as a function of minor radius, where the neutral hydrogen density has been set to zero in the calculation. The neoclassical slow rate illustrates the largest difference between the QHS and mirror configurations. For both the QHS and mirror configurations, the hybrid rate resides between the fast and slow rates.

The measured slow rise rates (r_s) are shown for the QHS and mirror configurations as a function of minor radius in Fig. 4. The measurements in the QHS configuration show a slower increase in the plasma flow compared to the mirror configuration, as expected for a configuration with reduced viscous damping. The calculated rates v_F are illustrated in the figure as well, and show good agreement with the data. The uncertainty in the calculated quantities is based on Monte Carlo propagation of the uncertainties in the measured plasma density, ion temperature, and neutral density. A measured neutral hydrogen density of $\sim 1 \times 10^{10}$ cm^{-3} was used in the calculation, leading to $v_{\text{in}} \approx 0.25$ kHz.
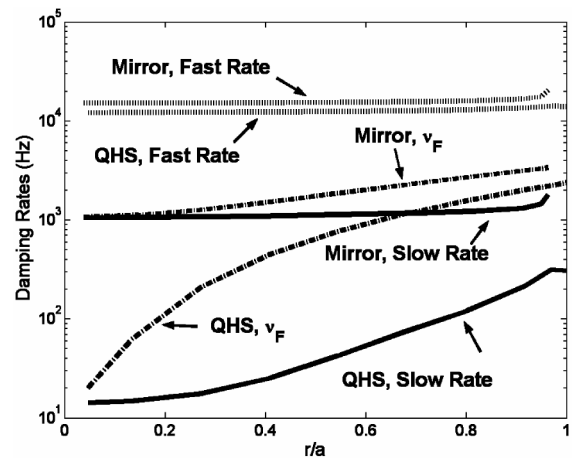
FIG. 3. Comparison of the calculated neoclassical damping rates for the QHS and mirror configurations.
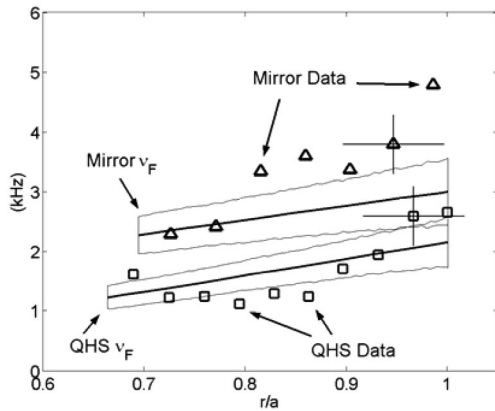
FIG. 4.   Measured slow flow spin-up rates in the QHS and mirror configurations and the theoretical rate ν_F.

FIG. 5.   Measured slow flow decay rates in QHS and mirror configurations and comparison to the slow decay rate of Eq. (5).

Note that the difference in the modeled predictions is due to neoclassical viscous damping, supporting the assertion that the measured difference is a neoclassical effect.

It was observed above that one component of the flows tends to decay at a rate of 30 kHz, which is similar to the decay rate of the floating potential. The rates for the slower flows to decay are illustrated in Fig. 5, for the QHS and mirror configurations of HSX. The flows decay more slowly in the QHS configuration, as anticipated for the configuration with reduced damping. The difference in damping rates is ~2–3 kHz. The neoclassical slow rate is also illustrated in the figure, for each of the two configurations. For the QHS configuration, this rate is mainly determined by ion-neutral collisions since the neoclassical viscous damping is so small. The rate at which the flows are damped is not consistent with neoclassical theory; the measurement and prediction differ by a factor of approximately 10 for the QHS case and 5 for the mirror. Note that the *difference* between the predictions of ~1.5 kHz is similar to the *difference* in the measurements. In this sense, we hypothesize that there may be an additional source of flow damping which tends to overwhelm most, but not all, of the predicted neoclassical difference. This result is in keeping with the results from axisymmetric systems, where it has been demonstrated in tokamaks [15] that the damping of plasma flows in the symmetry (toroidal) direction is anomalously fast.

In summary, two time scales are observed in the flow evolution, during both spin-up and spin-down, and techniques have been developed to extract these time scales from the Mach probe data. The rates for the flow to rise are in reasonable agreement with a model whereby the electric field formation initiates the spin-up of the plasma. The time to complete the spin-up is longer in the quasisymmetric configuration of HSX than a configuration where the quasisymmetry is broken, in agreement with neoclassical modeling. Although faster than neoclassical theory predicts, the measured slower rate for the flow to decay is reduced in the QHS configuration compared to the mirror. These results demonstrate for the first time that a quasi-symmetric stellarator has reduced neoclassical viscous flow damping.
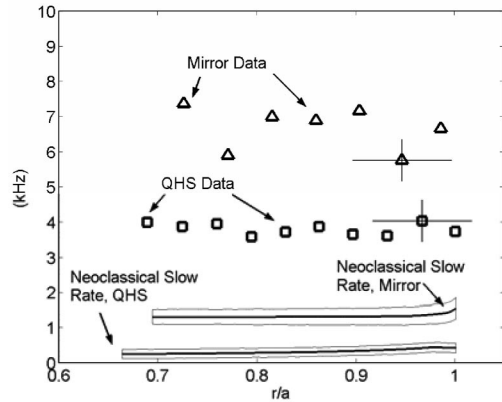
*Present address: Princeton Plasma Physics Laboratory, P.O. Box 451, Princeton, NJ 08543, USA.
[1] J. Nuhrenberg and R. Zille, Phys. Lett. A **129**, 113 (1988).
[2] M. C. Zarnstorff, *et al.*, Plasma Phys. Controlled Fusion **43**, A237 (2001); D. A. Spong *et al.*, Nucl. Fusion **41**, 711 (2001); S. Okamura *et al.*, Nucl. Fusion **41**, 1865 (2001).
[3] E. J. Synakowski *et al.*, Nucl. Fusion **39**, 1733 (1999).
[4] K. Ida and N. Nakajima, Phys. Plasmas **4**, 310 (1997).
[5] K. Ida *et al.*, in *International Conference on Plasma Physics, ICPP 1994*, edited by Paulo H. Sakanaka and Michael Tendler, AIP Conf. Proc. No. 345 (AIP, New York, 1995), p. 177.
[6] J. N. Talmadge *et al.*, in *Proceedings of the 15th International Conference on Plasma Physics and Controlled Fusion Research, Seville, 1994* (IAEA, Vienna, 1995), Vol. 1, p. 797.
[7] M. Coronado and J. N. Talmadge, Phys. Fluids B **5**, 1200 (1993).
[8] F. S. B. Anderson *et al.*, Fusion Technol. **27**, 273 (1995).
[9] W. D. D'haeseleer, W. N. G. Hitchon, J. D. Callen, and J. L. Shohet, *Flux Coordinates and Magnetic Field Structure* (Springer-Verlag, Berlin, 1991).
[10] S. P. Gerhardt *et al.*, Rev. Sci. Instrum. **75**, 4621 (2004).
[11] S. P. Gerhardt *et al.*, Rev. Sci. Instrum. **75**, 2981 (2004).
[12] K. C. Shaing, S. P. Hirshman, and J. D. Callen, Phys. Fluids **29**, 521 (1986).
[13] S. P. Hirshman, Nucl. Fusion **18**, 917 (1978).
[14] S. P. Gerhardt, Ph.D. dissertation, U. of Wisconsin-Madison, 2004.
[15] J. S. deGrassie *et al.*, Nucl. Fusion **43**, 142 (2003); L. G. Askinazi *et al.*, Nucl. Fusion **32** , 271 (1992).